

## RESEARCH ARTICLE

# Distinct targeting and uptake of platelet and red blood cell-derived extracellular vesicles into immune cells

Petra Ilvonen  | Reetta Pusa | Kai Härkönen | Saara Laitinen | Ulla Impola

Finnish Red Cross Blood Service, Helsinki, Finland

## Correspondence

Saara Laitinen, Research and Development,  
Finnish Red Cross Blood Service, Haartmaninkatu  
8, 00290 Helsinki, Finland.  
Email: saara.laitinen@bloodservice.fi

## Funding information

Business Finland, Grant/Award Number:  
2346/31/2019

## Abstract

Blood-derived extracellular vesicles (EVs) hold great therapeutic potential. As blood contains mixed EV populations, it is challenging to study EVs originating from different cells separately. Blood cell concentrates manufactured in blood banks offer an excellent non-invasive source of blood cell-specific EV populations. To study blood cell-specific EVs, we isolated EVs from platelet (TREV) and red blood cell (EryEV) concentrates and characterized them using nanoparticle tracking analysis, imaging flow cytometry, electron microscopy and western blot analysis and co-cultured them with peripheral blood mononuclear cells (PBMCs). Our aim was to use imaging flow cytometry to investigate EV interaction with PBMCs as well as study their effects on T-lymphocyte populations to better understand their possible biological functions. As a conclusion, TREVs interacted with PBMCs more than EryEVs. Distinctively, TREVs were uptaken into CD11c<sup>+</sup> monocytes rapidly and into CD19<sup>+</sup> B-lymphocytes in 24 h. EryEVs were not uptaken into CD11c<sup>+</sup> monocytes before the 24-h time point, and they were only seen on the surface of lymphocytes. Neither TREVs nor EryEV were uptaken into CD3<sup>+</sup> T-lymphocytes and no effect on T-cell populations was detected. We have previously seen similar differences in targeting PC-3 cancer cells. Further studies are needed to address the functional properties of blood cell concentrate-derived EVs. This study demonstrates that imaging flow cytometry can be used to study the distinctive differences in the interaction and uptake of EVs. Considering our current and previous results, EVs present a new valuable component for the future development of blood-derived therapeutics.

## KEYWORDS

blood cell, extracellular vesicle, imaging flow cytometry, platelet, red

## 1 | INTRODUCTION

Extracellular vesicles (EV) in plasma, and their involvement in intercellular communication in different physiological and pathophysiological conditions, as well as in immune responses by transferring their contents locally or systematically have been demonstrated by several studies (Danesh et al., 2014; Di Trapani et al., 2016; Kalluri & LeBleu, 2020; Mathieu et al., 2019; Parkkila et al., 2022; Pužar Dominkuš et al., 2018; Robbins & Morelli, 2014; Straat et al., 2016; Théry et al., 2009; Yáñez-Mó et al., 2015; Yates et al., 2022b; Yates et al., 2022a; Zhou et al., 2020). EVs are known to transfer surface receptors, mRNA, miRNA and signalling molecules intercellularly (Ratajczak et al., 2006; van der Pol et al., 2012) making them an ideal source of biomarkers (Ratajczak et al., 2006; Robbins & Morelli, 2014; Théry et al., 2002; van der Pol et al., 2012; Yáñez-Mó et al., 2015). The origin

Saara Laitinen and Ulla Impola contributed equally to this study.

This is an open access article under the terms of the [Creative Commons Attribution-NonCommercial-NoDerivs License](https://creativecommons.org/licenses/by-nc-nd/4.0/), which permits use and distribution in any medium, provided the original work is properly cited, the use is non-commercial and no modifications or adaptations are made.

© 2024 Finnish Red Cross Blood Service. *Journal of Extracellular Biology* published by Wiley Periodicals LLC on behalf of International Society for Extracellular Vesicles.

of EVs affects their cargo and further their functions, i.e. targeting, towards immune cells and may facilitate the penetration of the cargo through biological barriers such as the endothelial cell layer in hard-to-reach tissues like nervous tissue in the brain (Heidarzadeh et al., 2021; Puhm et al., 2021; Qu et al., 2018; Yates et al., 2022b; Yates et al., 2022a). Platelet-derived EVs and their role in haemostasis was one of the first functionally acknowledged characteristics for EVs reported in the literature over 70 years ago (Butler, 1989; Chargaff & West, 1946). During recent years, the immunological role of platelets has evoked scientific interest in addition to their well-described role in haemostasis (Aatonen et al., 2014; Jenne et al., 2013; Semple et al., 2011). Platelets communicate with immune cells and can promote the activation of neutrophils, monocytes and dendritic cells (Hottz et al., 2020; Passacuale et al., 2011; Semple et al., 2011). Interestingly, very recently, the immunological effects of RBCs have gained growing interest (Anderson et al., 2018; Laurén et al., 2022; Remy et al., 2018; Semple et al., 2011) and RBCs are shown to be involved in chemokine, nucleic acid and pathogen binding and can use haemoglobin release to generate reactive oxygen species (Anderson et al., 2018). However, the possible role of EVs in these immunological effects needs further investigation.

These yet partially unknown immunological roles of platelet and red blood cell (RBC) EVs have raised a growing interest in the possible immunological effects of blood product EVs. Both platelet concentrates (PC) and RBC units contain a huge number of different populations of blood-derived EVs which are even increased during the storage (Laurén et al., 2018; Valkonen et al., 2019) and then transfused to the patient within the product itself. With recent advances in technology, more precise characterization of the composition of PC- and RBC unit-derived EVs has become possible (Gamonet et al., 2017; Kuo et al., 2017; Thierry et al., 2015) but knowledge of their biological function, signalling and communication or targeting into other blood cells or tissues is still lacking (Arraud et al., 2014; Weiss et al., 2018). Few publications show that platelet EVs or RBC EVs seem to target certain mononuclear cell populations. One study found that platelet EVs interact with CD16+ monocytes (Weiss et al., 2018) and the same type of interaction was seen with RBC EVs and CD16+ monocytes by Danesh et al. (Danesh et al., 2014).

In this study, we assessed the interaction of the EVs isolated from RBC and PCs with primary peripheral blood mononuclear cells (PBMC) isolated from buffy coats. Using *in vitro* co-cultures and imaging flow cytometry techniques enabled us to investigate in detail, not only targeting but preciseness of the targeting, uptake and immunological consequences. We identified which cell sub-types interact with which EVs at multiple time points. We also looked if the studied EVs caused any changes in PBMC main populations using identifying surface markers and their combinations and further T-cells in an *in vitro* model used in clinical manufacturing quality assurance. The developed methods reported here can be used for further studies to reveal the underlying mechanisms behind the observed differences between cell-specific EVs and their targeting.

## 2 | MATERIALS AND METHODS

### 2.1 | Buffy coats and red blood cell and platelet concentrates

RBC concentrates, PC and buffy coats (BC) not needed for clinical use were obtained from the Finnish Red Cross Blood Service (FRCBS). PCs combined from four ABO and Rh-matched donors were stored at +20 to +24°C under constant agitation. RBC concentrates were stored at +2 to +6°C prior to use. In total, 18 blood products were utilized in this study. All donated blood products used for research were treated anonymously and were originally obtained from healthy volunteers who had given their informed consent. The research was in accordance with the rules of the Finnish Supervisory Authority for Welfare and Health (Valvira, Helsinki, Finland). Research permission was also obtained from the local Blood Service Board (Finnish Red Cross Blood Service, Finland).

### 2.2 | Isolation of mononuclear cells and cell culture

PBMCs were harvested from BCs and isolated using density gradient centrifugation (Ficoll-Paque plus, GE Healthcare). PBMCs were suspended into RPMI medium with 10% FBS (both Gibco) and counted using NucleoCounter (ChemoMetec). Cells were adjusted to a density of  $1 \times 10^6$  cells/mL and incubated at 37°C and 5% CO<sub>2</sub> on 48-well suspension cell plates (Greiner Bio-One).

### 2.3 | Isolation of extracellular vesicles

RBC concentrates (volume 260 mL) were diluted 1:1 with Dulbecco's phosphate-buffered saline (DPBS, Gibco) and centrifuged for 20 min at  $800 \times g$  at room temperature (RT) without brake and again at  $3000 \times g$  for 20 min at RT. PC (volume 244 mL) was diluted 1:2 with DPBS including 111:1000 of acid citrate dextrose (Terumo BCT). Samples were centrifuged for 7 min at  $650 \times g$  at RT without brake and again at  $1560 \times g$  for 20 min at RT. The supernatants were then filtered using SteriCup Filter Units with 0.22- $\mu$ m pore size (Merck) and further centrifuged at  $100,000 \times g$  for 1 h or 1.5 h at +4°C, respectively (with Optima™MAX-XP Ultracentrifuge with rotor MLA-50, k-factor 92, Beckman Coulter), washed with DPBS, and submitted into the second

ultracentrifugation at  $100,000 \times g$  for 1.5 h at  $+4^{\circ}\text{C}$  (in MLS-50 rotor, k-factor 71). The resulting platelet EV (TREV) pellets were thoroughly suspended in 200  $\mu\text{L}$  and RBC EV (EryEV) pellets in 400  $\mu\text{L}$  of DPBS. Samples were then centrifuged at  $3000 \times g$  for 10 min to remove any bigger aggregates. The supernatant was collected, aliquoted and stored at  $+4^{\circ}\text{C}$  until use.

## 2.4 | Characterization of EVs

### 2.4.1 | Nanoparticle tracking analysis

Particle concentration and size distribution were analysed with the nanoparticle tracking analysis (NTA) instrument ZetaView PMX-120 (ParticleMetrix). Upon measurements, camera and laser alignment were optimized and auto-symmetry was carried out. EV samples were diluted in milli-Q to 50–200 particles per frame. Samples were analysed from 11 positions, with a camera sensitivity of 85, a shutter speed of 100, medium video quality at 30 frames/s rate, minimal area of 10 and maximal area of 1000. The temperature was set to  $22^{\circ}\text{C}$ . Data were analysed with instrument software (Software ZetaView version 8.05.12 SP2).

### 2.4.2 | Scanning electron microscopy

Fifteen microlitres of EV sample was added to Concanavalin A-coated coverslips, fixated with 5% glutaraldehyde in 100-mM NaCitrate-2, incubated 30–60 min at RT and washed twice with 100-mM NaCitrate-phosphate buffer. Samples were osmicated with 1%  $\text{OsO}_4$  water for 30–60 min, washed twice with 100-mM NaCitrate-phosphate buffer and dehydrated with an ethanol series. Hexamethyldisilazane was added and samples were dried overnight. A conductive bridge was made with Agar Silver Paint (Agar Scientific). Samples were coated with 5-nm platinum using Quorum Q150T S sputter (Quorum Technologies Inc.) and imaged with FEI Quanta FEG 250 scanning electron microscope at 10–15 kV.

### 2.4.3 | Cryo-electron microscopy

The sample was vitrified on Quantifoil R1.2/1.3 holey carbon grid using a Leica EM GP plunger set at 80% humidity and 1.5-s blotting time and imaged using Talos Arctica transmission electron microscope (Thermo Fisher Scientific) equipped with a Falcon III direct electron detector (Thermo Fisher Scientific).

### 2.4.4 | Western Blot analysis

The sample protein content was determined using Pierce BCA Protein Assay Kit (Thermo Fisher Scientific). Samples containing 5  $\mu\text{g}$  of protein and 1/4 of 4X Laemmli buffer (Bio-Rad) were loaded onto Mini-Protean TGX 4%–20% gels (Bio-Rad) and run at 40 V for 10 min and 200 V for 35 min in 1 $\times$  Tris/Glycine/SDS Buffer (Bio-Rad). Semi-wet transfer was done using Trans-Blot Turbo (Bio-Rad) (with settings: 2.5 A, up to 25 V, 3 min), 1 $\times$ TransBlot<sup>®</sup> Transfer Buffer (Bio-Rad) with 20% ethanol and TransBlot<sup>®</sup> Turbo<sup>™</sup> Mini-size PVDF Membrane (Bio-Rad). The membrane was blocked in 3% BSA (Biowest).

Primary antibodies CD235a (BD Pharmingen), CD9, CD63, ApoA1 and ApoB (all Medix Biochemical) were diluted 1:1000 and CD41 (Beckman Coulter) 1:10,000 in 3% BSA in TBS-T (Tris-buffered saline with 0.1% Tween-20). Membranes were incubated at  $+4^{\circ}\text{C}$  overnight and washed with TBS-T for 10 min three times. Goat Anti-Mouse IgG (Bio-Rad) was diluted to 1:500 and Streptactin-HRP Conjugate (Bio-Rad) 1:5000 in TBS-T as the secondary antibody solution. The membranes were incubated for 1 h at RT and washed with TBS-T for 10 min three times and finally in TBS for 5 min. Clarity<sup>™</sup> Western ECL Substrate (Bio-Rad) was mixed and added on top of the membrane fractions and incubated at RT for 1 min. Chemiluminescence was measured using the ChemiDocTouch Imaging System (Bio-Rad).

### 2.4.5 | Amnis<sup>®</sup> ImageStream X Mark II analysis of extracellular vesicles

Identities of blood product-derived EVs were verified using antibodies against erythrocyte Glycophorin A (CD235a) (clone: 11E4B-7-6, Beckman-Coulter), platelet transmembrane glycoprotein CD41 (clone: HIP8, BioLegend) and CD9 (clone: MEM-61, Abcam) which is a general marker of exosomes.  $1 \times 10^8$  particles according to the NTA results in a total volume of 50  $\mu\text{L}$  were labelled for 60 min at RT in the dark. Because of the background of CD9 fluorochrome aggregates, the antibody was first diluted 1:15 in DPBS and centrifuged at  $16000 \times g$  for 10 min after which the supernatant was used for labelling (Tertel et al., 2020). Sample buffer, antibody-only, unlabelled and 0.2% Triton X-100 treated EVs were used as controls.

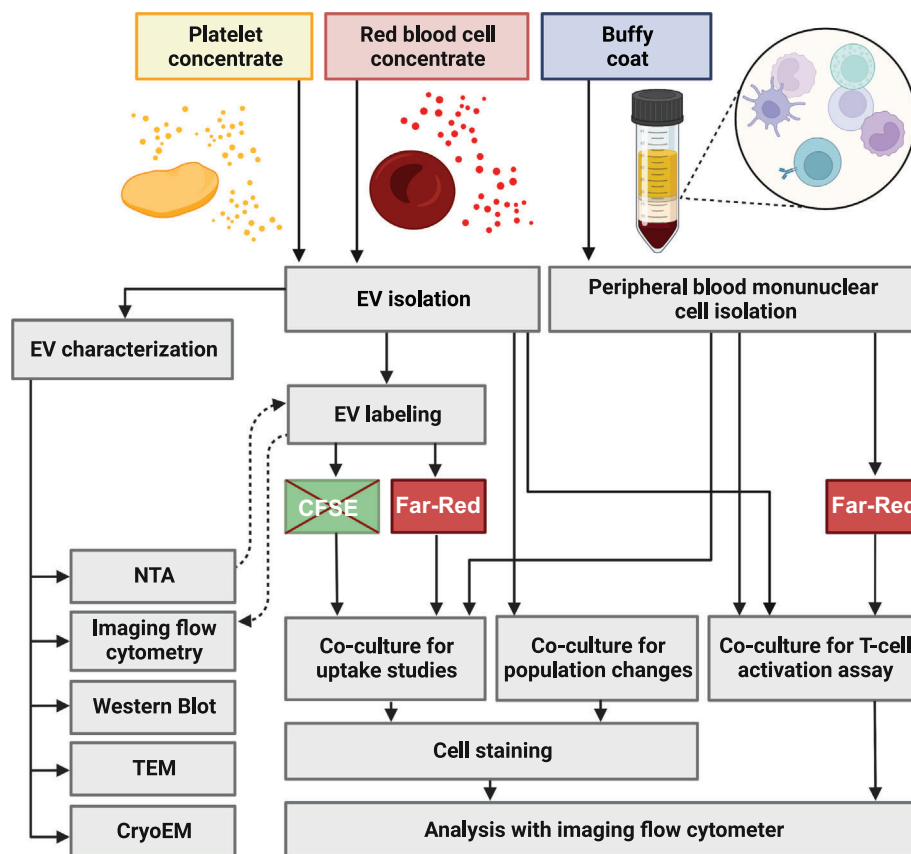


**FIGURE 1** Schematic design of the study illustrating the materials and methods used and highlighting the most significant steps in the workflow of this study. CFSE, ((5(6)-CFDA, SE; CFSE (5-(and-6)-carboxyfluorescein diacetate, succinimidyl ester; CryoEM, cryogenic electron microscopy; EV, extracellular vesicle; Far-Red, Far-Red CellMask labelling; NTA, nanoparticle tracking analysis; SEM, scanning electron microscopy. Figure created in Biorender.

Labelled EV samples were characterized using Amnis® ImageStream®X Mk II Imaging Flow Cytometer (Luminex/Cytek Biosciences). Excitation lasers 488, 642 and 785 nm were used with maximum voltages. Channels Ch01 and Ch09 were used for the bright field (BF), Ch06 for side scattering and channels Ch02 and Ch011 for fluorescence signal detection. Amnis® High Gain Mode and 60× magnification were used for enhanced small particle detection. All data were analysed using IDEAS® 6.2 Image Data Exploration and Analysis Software following methods described in Görgens et al. (2019).

## 2.5 | EV co-culture with peripheral mononuclear cells

For internalization studies, EV samples were labelled with fluorescent molecules. As described earlier, we also noticed that PBMCs show significant autofluorescence on the emission wavelengths excited by 488 nm but not on higher wavelengths (Mitchell et al., 2010). Therefore, the first tested CFSE ((5(6)-CFDA, SE; CFSE (5-(and-6)-Carboxyfluorescein Diacetate, Succinimidyl Ester), which was excited with 488-nm laser was exchanged for a Far-Red CellTrace Kit, which contains a similar cell-permeant non-fluorescent ester of an amine-reactive fluorescent molecule that is converted to a fluorescent derivative by esterases when inside the cell or vesicle and excited with 642-nm laser (CellTrace™ Far-Red Cell Proliferation Kit, Invitrogen). EVs were labelled with 20- $\mu$ M CFSE or Far-Red molecules for 15 min at 37°C. Excess free-label molecules were purified using Exosome Spin Columns (Invitrogen). Samples with fluorochrome labels without EVs (MOCK) as well as only DPBS were performed in parallel fashion to get background controls and confirm the excess dye retention by columns.

The workflow of the study is illustrated in Figure 1. PBMCs in a density of  $1 \times 10^6$  cells/mL in a total volume of 0.5 mL/well were co-cultured with  $1 \times 10^{10}$  labelled or unlabelled EVs, MOCK or DPBS controls on 48-well suspension cell plate (Greiner Bio-One). For internalization studies, labelled EVs were co-cultured for 30 min, 2 h and 24 h. Possible cell population changes after administration of unlabelled EVs were analysed after 96 h of co-culture. Triplicates of each sample type and timepoint were combined for cell labelling. After incubation cells were collected and centrifuged at  $300 \times g$  for 7 min in RT, and the media was replaced with cold 2% FBS-DPBS. Different cell populations were identified using mainly the same combinations of fluorochrome-labelled antibodies as described in Impola et al. (2016).

## 2.6 | T-cell activation assay

Forty-eight-well suspension cell plates were coated using CD3 (Sanquin) diluted to 1  $\mu\text{g}/\text{mL}$  and incubated at 37°C and 5% CO<sub>2</sub> for 2 h. The PBMCs were isolated, counted and diluted to 1  $\times 10^6$  cells/mL in 0.1% FBS-DPBS and labelled using CellTrace™ Far-Red Cell Proliferation Kit (Invitrogen). Cells were labelled in RT in the dark for 20 min and then washed using 0.1% FBS-PBS three times. Finally, they were diluted to 1  $\times 10^6$  cells/mL according to the previous cell count. Unlabelled cells were plated for control.

Cells in 0.5 mL were administered with 1  $\times 10^{10}$  unlabelled TREVs or EryEVs, in both CD3-coated wells and uncoated wells. This experiment was done with TREVs and EryEVs suspended to DPBS in a concentration of 2  $\times 10^{10}$  particles/mL, snap-frozen in liquid nitrogen and stored at -80°C for 2 months. As positive controls, we used CFSE-labelled cells in wells coated with CD3 alone or together with CD28 (Sanquin). DPBS-treated and untreated cells were used as negative controls. Cells were incubated at 37°C and 5% CO<sub>2</sub> for 5 days. Triplicates of the same sample type were combined and centrifuged at 300  $\times g$  for 7 min at RT and media was replaced with cold 2% FBS-DPBS.

## 2.7 | Analysis of mononuclear cell populations with Amnis® ImageStreamX Mark II

Mononuclear cells were identified using fluorescently labelled surface markers and were analysed with a 12-channel Amnis® ImageStream<sup>®X</sup> Mark II (Luminex, Cytex Biosciences) imaging flow cytometer. Samples were acquired at 60 $\times$  magnification with a low flow rate/high sensitivity. The integrated software INSPIRE® (Luminex, Cytex Biosciences) was used for data collection. The instrument and INSPIRE® software were set up as follows: Excitation lasers 405 (10 mV), 488 (200 mV), 642 (120 mV) and 785 (2 mV). Channels Ch01 and Ch09 were used for brightfield (BF) and Ch06 or Ch12 for scattering signals. All other channels were activated for fluorescence signal detection if needed. Single colour controls were used for compensation and unlabelled cells, or cells incubated with unlabelled EVs or MOCK label were used to determine autofluorescence and background. Compensated data files were analysed using image-based algorithms available in the IDEAS® statistical analysis software package (version 6.2.188.0). Positive events for different fluorophores were gated based on the intensity values on each channel and images. We also used image-based analysis to determine the internalization of the fluorescent signal. This was based on the software internalization feature and a masking tool which can calculate and verify if the Far-Red signal from labelled EVs is coming from the cell membrane or inside the cell. The use of IDEAS® software algorithms in this kind of studies was mimicking the methods described earlier by other groups (Görgens et al., 2019; Hewitt et al., 2017; Jurgielewicz et al., 2020; Park et al., 2020).

For the T-cell activation assay, the instrument and INSPIRE® software were set up as follows: excitation lasers 488 (200 mV), 642 (10 mV) and 785 (2 mV). Channels Ch01 and Ch09 were used for brightfield (BF) and Ch06 for scattering detection. Ch03 and Ch11 were activated for fluorescence signal detection. CD3+ cells, labelled with CD3 PE (Invitrogen) were used for gating and 5000 lymphocytes were collected per sample. After proliferation, the intensity of the CellTrace signal from a new cell generation is in theory halved compared to the parent population, so the number of different intensity peaks was counted and gated based on the mean intensities of these new cell generations as described also by Kit manual.

## 2.8 | Statistics

All datasets were analysed using GraphPad Prism 9.5.1. (San Diego, California). The data are presented as mean  $\pm$  standard deviation as reported. Statistical significance was determined using the Wilcoxon test for comparison between paired samples, Mann–Whitney  $U$  for comparison between unpaired samples, and a  $p$ -value under 0.05 was considered significant.

# 3 | RESULTS

## 3.1 | Characterization of EVs

### 3.1.1 | EryEVs are bigger in size and their shape is more tubular than TREVs

Particle amount and size from TREV and EryEV samples were measured using NTA from multiple biological replicates. The mean total number of particles in TREV samples was 1.2  $\times 10^{12}$  (SD  $\pm$  2.3  $\times 10^{11}$ ,  $n = 6$ ), and in EryEV samples 8.7  $\times 10^{11}$  (SD  $\pm$  5.0  $\times 10^{11}$ ,  $n = 6$ ). There is no statistical significance in the total number of particles between the sample types ( $p = 0.372$ ). Most particles were under 200 nm in both sample types, the mean particle size in TREV samples was 126 nm (SD  $\pm$  9.9 nm,  $n = 6$ ) and in EryEVs 185 nm (SD  $\pm$  11.3 nm,  $n = 6$ ). The mean difference was also reflected in the distribution of the particle sizes in each sample as illustrated in Figure 2a. The difference in particle size between TREVs and EryEVs was also confirmed with

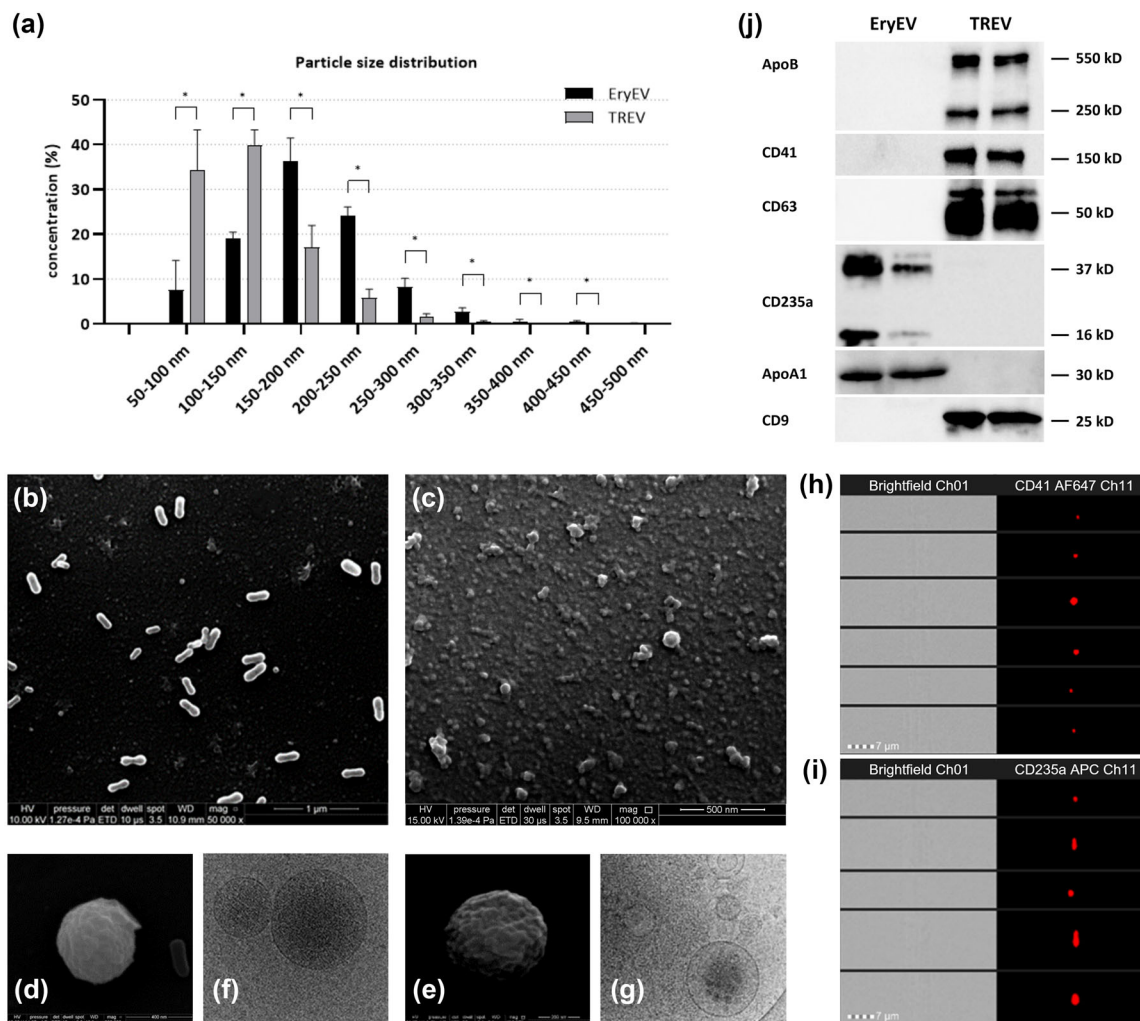


**FIGURE 2** EV characterization using nanoparticle tracking analysis, western blotting, scanning electron microscopy (SEM), cryogenic electron microscopy (cryoEM) and imaging flow cytometry. (a) Particle size distribution measured with the Zetaview PMX-120 (ParticleMetrix). The mean particle size in TREV samples was 126 nm (SD  $\pm$  9.9 nm,  $n$  = 6 biological replicates) and in EryEVs 185 nm (SD  $\pm$  11.3 nm,  $n$  = 6 biological replicates). There is a significant difference in particle size distribution between TREVs and EryEVs. (b–e) Scanning electron microscopy images illustrate the size and shape difference between EryEVs (b and d) and TREVs (c and e), the tubular shape of EryEVs is highlighted. Original magnifications are  $\times$ 50,000 in (b),  $\times$ 100,000 in (C) (scale bar 1  $\mu$ m),  $\times$ 200,000 in (d) (scale bar 400 nm) and  $\times$ 250,000 in (e) (scale bar 200 nm). (f–g) Cryogenic electron microscopy images that show the lipid bilayer composition on single vesicles in (f) EryEV and (g) in TREV samples. (h, i) Representative panels from imaging flow cytometry images of (h) CD41-labelled (AF647, Biolegend) TREVs and (i) CD235a-labelled (APC, BD Bioscience) EryEVs and their corresponding brightfield images. (j) Western blot analysis shows that ApoB48, ApoB100 (both bands), CD9, CD41 and CD63 were present in TREV samples while ApoA1 and CD235a were absent and were detected only in EryEV samples.

Amnis® ImageStreamX Mark II side scatter signal using a 785-nm laser and from SEM pictures as seen in Figure 2b–e. TREVs are generally spherical and EryEVs are often tubularly shaped as shown in Figure 2b,c. Amnis images from fluorochrome-conjugate anti-CD235a antibody labelled EVs also illustrate this as seen in Figure 2i. The surface of TREVs is rougher and a corona-type surface is seen on some vesicles as pictured in Figure 2d. TREV samples contain more contaminating background particles, that can also affect the corona formation. Cryo-EM images of single vesicles show the lipid bilayer composition pictured in Figure 2f,g. The differences in shape that were observed in SEM images were not seen in Cryo-EM images.

### 3.1.2 | Characteristic EV and specific glycoprotein markers indicate the purity of TREVs and EryEVs

Tetraspanin CD9 and CD63 proteins were detected in TREV samples, but not in EryEV samples by western blot analysis as illustrated in Figure 2j. Also, the transmembrane glycoprotein CD41 which was used as a marker for platelet origin was detected only in TREV samples both with western blot and with a flow cytometry analysis as expected. EryEVs did not show any CD41 or CD9 signal but were positive for CD235a on western blots (see Figure 2j) and 60%–90% of EryEV small particles were positive

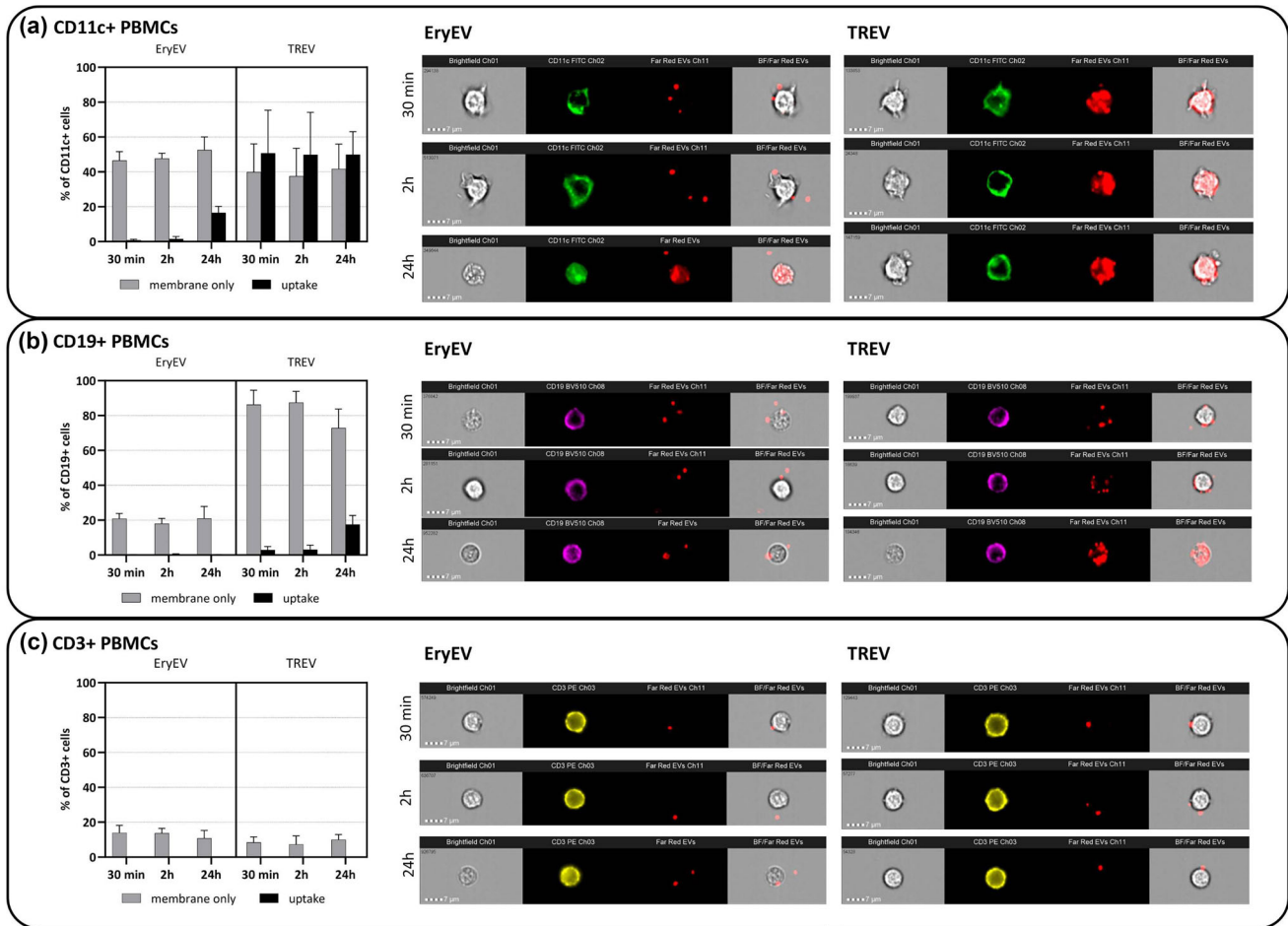


**FIGURE 3** EV interaction and uptake with peripheral blood mononuclear cells (PBMCs). EVs labelled with Far-Red CellTrace. Most interaction was seen between TREVs and CD11c+ monocytes (a).  $0.5 \times 10^6$  PBMCs were administered with  $1 \times 10^{10}$  Far-Red-labelled TREVs or EryEVs. Cells were identified using CD11c FITC (Invitrogen), CD19 Bright Violet 510 (BioLegend) and CD3 PE (Invitrogen) and analysed with Amnis® ImageStreamX Mark II imaging flow cytometer (Luminex). (a) Shows EV interaction with CD11c+ cells, (b) interaction with CD19+ B-lymphocytes and (c) interaction with CD3+ T-lymphocytes. (a–c) show the percentage of cells that have EVs either only on the membrane or also uptaken into cells. Data are presented as mean  $\pm$  SD,  $n = 4$ . Representative image panels from Amnis® ImageStreamX Mark II imaging flow cytometry, showcasing a brightfield image on Ch01, fluorescently labelled cells from Ch02, Ch03 and Ch08, Far-Red-labelled EVs on Ch11 and a merged image to illustrate EV interactions in different cells after either 30 min, 2 h or 24 h of co-culture.

for CD235a. This indicates that RBC concentrates, and RBC EVs have no detectable amount of platelet-derived CD41+ EVs as impurities. However, they do contain CD235a negative particles, indicating that particles other than RBC origin are present in the sample. Both, ApoB 48 and ApoB 100, bands can be seen on TREV samples by western blot but ApoA1 on the other hand was only seen on EryEV samples and not in TREVs as pictured in Figure 2j.

## 3.2 | EV interaction and uptake into different immune cells

### 3.2.1 | TREVs are rapidly uptaken into CD3–/CD11c+ monocytes

Both TREVs and EryEVs were interacting with CD3–/CD11c+ monocytes. From TREV-treated samples, a Far-Red signal from inside CD11c+ monocytes was detected at all time points. The difference between TREVs and EryEVs in uptake is best illustrated by the figure panel in Figure 3a. Of CD11c+ cells 50.7% (SD  $\pm$  24.6%) at 30 min, 49.8% (SD  $\pm$  24.4%) at 2 h, and 49.9% (SD  $\pm$  13.2%) at 24 h had Far-Red labelled EVs inside as presented in Figure 3a. EryEV-treated samples had Far-Red signal mainly on the cell membranes at all time points, 46.6% (SD  $\pm$  5.1%) at 30 min, 47.7% (SD  $\pm$  3.0%) at 2 h and 52.5% (SD  $\pm$  7.5%) at 24 h as presented in Figure 3a. After 24 h of co-culture with EryEVs, a Far-Red signal was also detected inside 16.6% (SD  $\pm$  3.7%) of CD11c+ cells. No statistically significant differences between time points of the same group were observed. Altogether there was

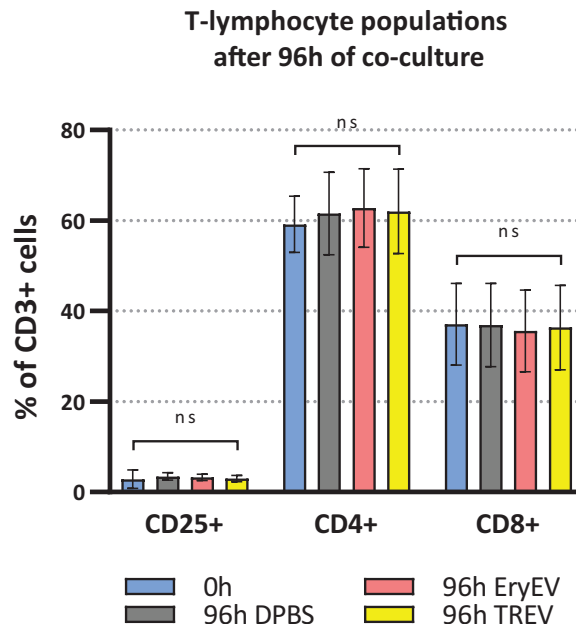


**FIGURE 4** EVs have no effects on main T-cell populations under 4-day co-culture. Percentage of CD4+, CD8+ or CD25+ cells of CD3+ T-lymphocytes presented as mean  $\pm$  SD, ( $n = 6$  for TREVs and EryEV treated samples and  $n = 3$  for DPBS control and 0-h sample). Measured with Amnis® ImageStreamX Mark II imaging flow cytometry. No significant changes were seen, determined with multiple Whitney–Mann  $U$  tests, ns =  $p$ -value over 0.05.

significantly less uptake with EryEVs and CD11c+ monocytes than with TREVs at 30 min ( $p = 0.029$ ), 2 h ( $p = 0.029$ ) and 24 h ( $p = 0.029$ ).

### 3.2.2 | EryEVs were uptaken into CD3<sup>-</sup>/CD19<sup>+</sup> B-lymphocytes only after 24 h

TREVs and EryEVs interact differently with CD3<sup>-</sup>/CD19<sup>+</sup> B-lymphocytes, illuminated by the figure panel in Figure 3b. TREV-treated CD3<sup>-</sup>/CD19<sup>+</sup> B-lymphocytes had the Far-Red signal at the earlier time points mostly on the cell membranes 86.2% (SD  $\pm$  8.3%) at 30 min, 87.4% (SD  $\pm$  6.4%) at 2 h and 72.8% (SD  $\pm$  10.9%) at 24 h (see Figure 3b). After 24 h co-culture, 17.5% (SD  $\pm$  4.5%) of B-lymphocytes had a Far-Red signal inside the cell. In contrast, EryEVs were only detected on the surface of CD19<sup>+</sup> B-lymphocytes at all time points, 20.9% (SD  $\pm$  3.0%) at 30 min, 18.1% (SD  $\pm$  2.9%) at 2 h and 21.0% (SD  $\pm$  6.9%) at 24 h as presented in Figure 3b. There was statistically more uptake of TREVs than EryEVs to CD19<sup>+</sup> B-lymphocytes at 30 min ( $p = 0.029$ ), 2 h ( $p = 0.029$ ) and 24 h ( $p = 0.029$ ). Significant differences in the interaction seen on the membrane were observed at 30 min ( $p = 0.029$ ) and 24 h ( $p = 0.029$ ), but not at 2 h ( $p = 0.114$ ).

### 3.2.3 | CD3<sup>+</sup> T-lymphocytes showed little interaction with TREVs and EryEVs

Some Far-Red-labelled EVs were observed near CD3<sup>+</sup> T-lymphocytes and on the cell membrane, but there were no statistical differences between the sample types. The scarcity of interaction between both EV types and CD3<sup>+</sup> T-lymphocytes is imaged on the figure panel in Figure 3c. On average, 8.5% (SD  $\pm$  3.6%) of the TREV-treated CD3<sup>+</sup> T-lymphocytes were positive for Far-Red signal on the cell membrane at all time points as seen in Figure 3c. Of EryEV-treated samples, there was no statistical difference between time points, and on average, 12.8% (SD  $\pm$  3.9%) of T-lymphocytes were positive for Far-Red signal on the cell membrane as shown in Figure 3c.

## 3.3 | TREVs and EryEVs do not affect the composition of mononuclear cell populations in co-culture

The percentage of the CD3<sup>+</sup> T-cell population remains unchanged after a 4-day co-culture with TREVs and EryEVs when compared to controls. As illustrated in Figure 4, the proportions of T-cell subpopulations, including CD25+, CD4+ and CD8+ cells, exhibited no discernible changes in response to co-culturing with either EryEVs or TREVs. In addition, no apparent changes in

### Lymphocyte proliferation determined by Far-Red intensity

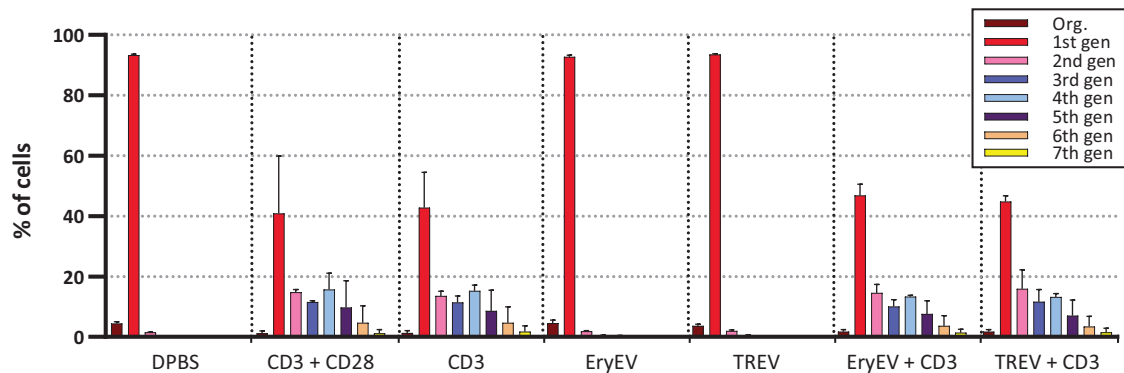


**FIGURE 5** EVs have no effects on lymphocyte proliferation. After a 5-day co-culture, proliferation of lymphocytes was determined by Far-Red CellMask proliferation dye intensity. Measured with Amnis® ImageStreamX Mark II imaging flow cytometry. In theory, the intensity of each generation is half of the previous generation and the proliferation rate was studied by gating each generation. CD3 antibody-coated plates were used to see if EVs had inhibitory effects, CD3 antibody-coated wells as such and with CD28 antibody were used as positive controls, and DPBS-treated wells as negative control. TREV or EryEV treatment does not affect proliferation by either activating or inhibiting it.

the proportions of CD56+, CD123+ and CD19+ cells were seen. Some differences in cell ratios occur due to biological differences between donors of PBMCs.

### 3.4 | TREVs or EryEVs do not activate nor affect T-cell activation in standard *in vitro* assay

We see no increase in T-cell proliferation indicating that there is no activation in samples treated solely with EryEVs and TREVs as compared to untreated control cells as presented in Figure 5. This lack of T-cell activation in response to EryEVs and TREVs alone suggests that these vesicles do not possess inherent stimulatory properties under our experimental conditions. The samples that were given EryEVs or TREVs together with CD3 have similar T-cell proliferation rates as positive controls treated with only CD3 or both CD3 and CD28 as presented in Figure 5. Thus, EV samples do not have an inhibiting effect on cell proliferation either. Individual differences between PBMC donors were seen, but no relation to the treatment was identified.

## 4 | DISCUSSION

Both platelets and more recently RBCs have been studied for their immunological effects and interactions with immune cells (Butler, 1989; Caillon et al., 2022; Ebeyer-Masotta et al., 2022; Hemler, 2005; Kowal et al., 2016; Noris & Galbusera, 2023; Weiss et al., 2018; Yan et al., 2023). Further, EVs from platelet and RBCs in blood and plasma have been proposed to be key players in intercellular signalling and modulate immune responses in their microenvironment, especially by triggering signalling pathways but also directly by transferring receptors and inflammatory mediators from cell to cell (Danesh et al., 2014; Kuo et al., 2017; Mantel et al., 2016; Straat et al., 2016; Yáñez-Mó et al., 2015). The cellular origins of EVs affect their surface markers, lipid composition and molecular cargo, which can influence their immunological functions and targeting efficiency (Puhm et al., 2021; Yates et al., 2022b; Yates et al., 2022a). Isolation of EVs from plasma has major challenges as they contain a mix of blood cell-derived vesicles, lipoprotein particles, and other proteins as impurities or co-isolates (Onódi et al., 2018). These co-isolates can complicate the study of the biological role of platelet or RBC EVs. We tried to overcome this problem by harvesting EVs directly from blood cell concentrates that are enriched for specific blood cell EVs and contain less plasma compared to whole blood samples. We aimed to further understand the interaction, targeting and uptake of TREVs and EryEV to mononuclear cells.

Characteristically, the mean size of EryEVs was bigger and they showed more tubular shapes in SEM images when compared to smaller and round TREVs. This tubular shape of EryEVs has been described also previously (Arraud et al., 2014; Kralj-Iglič et al., 2020; Laurén et al., 2022) and it can affect the accuracy of NTA measurements, as the calculations are based on Brownian motion and assume spherical shape (Dragovic et al., 2011). Only TREVs were positive for CD9 and CD63 tetraspanins and CD41 whereas EryEVs lacked all these markers but were positive for CD235a. As shown, already, earlier by our group (Laurén et al., 2018), we also now confirmed with western blots that EryEVs from RBC units are positive for ApoA1 whereas TREVs on the other hand were only positive for ApoB. The ApoA1 signal in EryEVs might originate from the protein corona of EVs or from apolipoproteins co-isolated with EVs (Palviainen et al., 2020; Tóth et al., 2021). However, the absence of ApoA1 in TREV samples isolated from PCs containing more plasma does not support the latter notion. It has been suggested that EryEVs take part in the

RBCs role in reverse cholesterol transportation, but the mechanisms involved are still unclear (Dergunov & Baserova, 2022; Lai et al., 2019). Lai et al. (2019) concluded that ApoA1 transports cholesterol to RBCs unidirectionally and that the transportation of cholesterol between HDL and RBCs is bidirectional. These interactions could explain the ApoA1 signal from EryEVs; however, further studies are needed to characterize EV involvement in cholesterol transportation.

In previous studies, platelet or RBC EVs isolated from plasma seemed to interact mainly with CD14+ and CD16+ monocytes (Danesh et al., 2014; Weiss et al., 2018) which most likely are circulating dendritic cells as the majority of them are CD14+ and can also be CD16+ (MacDonald et al., 2002). Straat et al. (2016) reported that labelled RBC-derived EVs bind and are phagocytosed into monocytes, and they also saw a reduction in interaction when monocytes were first incubated with anti-CD11b and anti-CD18 antibodies which suggested that this interaction involves adherence to monocytes. These results were based on confocal imaging and conventional flow cytometric analysis. Using imaging flow cytometry, we could separate between membrane binding and uptake into the cell in more detail and we can confirm the adherence to monocytes, but we saw uptake of EryEVs only after 24 h. Weiss et al. (2018) reported interactions between CD235+ EVs of RBC-origin and leucocytes were scarcely detectable and saw that platelet EVs are more associated with monocytes and granulocytes but rarely detected with lymphocytes. We reported that the majority of the TREVs and EryEV interaction was seen with CD3−/CD19−/CD11c+ cells which are mostly considered to be monocytes, conventional/monocyte-derived dendritic cells or macrophages (Sozzani et al., 2017). Thus, we can confirm the general preference to interact with monocytes, but we also show strong interactions with CD19+ B-lymphocytes.

Overall, we saw more interaction between TREVs and PBMCs than between EryEVs and PBMCs. One explanation could be the smaller average size of TREVs which could facilitate their uptake (Mulcahy et al., 2014). While size can play a crucial role, our findings indicate that uptake is not solely determined by size, as also EryEVs contain a substantial number of smaller particles that would be then taken up similarly to TREVs if the size would be the only determinant. A recent study compared small and medium EVs from murine plasma and reported no significant difference between their *in vivo* distribution or differences depending on EV size on uptake into hepatocytes *in vitro*, but did see differential uptake into different cells in co-culture model (Németh et al., 2021). As for the shape of EryEVs and its possible role in uptake, this can only be speculated as one factor. Another contributing factor could be the presence of tetraspanins on TREV membranes which might ease their uptake into PBMCs because of their known involvement in adhesion and migration (Hemler, 2005). A larger variety of tetraspanins on TREV membranes might also add options for different adhesion and uptake routes (Liu & Wang, 2023; Mulcahy et al., 2014). It has also been shown that there is CD47 present on EryEVs especially when isolated from older RBC concentrates (Gamonet et al., 2020; Stachurska et al., 2019). CD47 is known to inhibit macrophages from phagocytosing (Burger et al., 2012) the RBCs so it could be one factor contributing to lower uptake of EryEVs. In addition, the lesser interaction of EryEVs and cells could be explained by the possible cytotoxic effect of denatured haemoglobin that we have previously shown to be present in EryEVs (Laurén et al., 2018). A similar mechanism is seen in RBCs, which can release heme and haemoglobin and create toxic reactive oxygen species as part of the host immune defence (Anderson et al., 2018).

Interestingly, in addition to the eagerness to interact with different monocytes, also the kinetics of EV uptake into different cells varied between EryEVs and TREVs. In comparison, TREV-treated PBMC samples had a higher number of EVs in CD3−/CD11c+ monocytes and the uptake of them was quicker than EryEVs which were uptaken only after 24 h. Also, the number of EVs in CD3−/CD19+ B-leucocytes was significantly higher in TREV-treated than EryEV-treated PBMCs. The same kind of difference in the uptake of EryEVs and TREVs by PC-3 prostate cancer cells was seen in our earlier study by Koponen et al. (2020). Adherent PC-3 cells were studied using surface plasmon resonance, confocal imaging and flow cytometry, and all methods showed more interaction between TREVs and PC-3 cells when compared to EryEVs. Koponen et al. (2020) also reported that the cellular uptake of TREVs was significantly faster than that of EryEVs. So the differences between TREV and EryEV targeting seem to be fundamental as similar observations were seen previously with adherent cancer cells and with healthy haematological cells as reported here. We understand that when we detect the internalized signal, we cannot rule out the possibility that instead of the intact EV, the fluorescent signal might originate from an EV which has fused with the cell membrane and deliberated its cargo together with the fluorescent label inside the cell. Nevertheless, this is also as important finding as the internalization of the intact EV itself.

Several earlier studies have shown that blood EVs have inflammatory effects (Danesh et al., 2014; Weiss et al., 2018). Based on our results, the studied EVs seem to have no significant immunological effects on T-cells *in vitro*. Danesh et al. (2014) used RBC-derived EVs to study PBMC survival and T-cell responses and concluded that RBC-derived EVs could stimulate PBMCs and provoke proinflammatory cytokine response. The authors in Danesh et al. (2014) hypothesized that the EV-induced T-cell proliferation was mediated by antigen-presenting cells (APC). This report led us to use the PBMC population including possible APCs and not isolated T-cells in this study. Although we saw no effect on T-cell proliferation, the suggestion for APC-dependency is supported by our findings on EV uptake into CD11c+ cells known to act as APCs as well as no uptake seen on CD3+ T-lymphocytes. Also, our recent study showed that diluted residual plasma isolated from RBC units caused T-cell proliferation *in vitro*, whereas a similar effect was not seen with EryEVs (Laurén et al., 2022).

Comparison with older studies is difficult due to the variability in study design and development of EV isolation and characterization protocols in recent years. When we use imaging flow cytometry, we are also able to follow the fluorescent signal of EVs in a suspension cell population, which would be otherwise difficult. The rapid development of more precise and sensitive

imaging flow cytometers has also allowed the characterization of smaller particles under 300 nm<sup>38</sup>. This has required careful method development, especially with different labelling techniques to avoid misinterpretation of the results. Especially in uptake studies, the selection of the used labelling techniques and fluorochromes is crucial as some cells show substantial autofluorescence on the lower wavelengths (Shrirao et al., 2021) as seen in our Appendix Figure 1. Widely used green fluorochromes excited by 488 nm such as FITC and AF488 may be particularly challenging to analyse potentially leading to false interpretation in EV targeting and uptake studies.

We can conclude that there is significantly more interaction between TREVs and PBMCs compared to EryEVs and PBMCs. Most interactions were seen with CD11c+ cells and some with CD19+ cells indicating their possible role in the antigen presentation process. TREVs are taken into CD11c+ monocytes quickly and into CD19+ B-lymphocytes after 24 h of co-culture. EryEVs are seen on the cell membranes of both CD11c+ and CD19+ cell populations and are only uptaken into CD11c+ monocytes after 24 h of co-culture. Neither TREVs nor EryEVs influence the T-cell population or proliferation *in vitro*. We realize that this *in vitro* study cannot replicate *in vivo* studies and concentrates only on a portion of all cell types co-operating in the blood stream *in vivo*. However, using the population of all mononuclear cells harvested from the fresh blood, we believe that we are still able to see the effect of EVs on most of these cell types. Further studies on this subject are needed to describe EV and PBMC interactions and mechanisms in more detail and to determine *in vivo* relevancy.

## AUTHOR CONTRIBUTIONS

**Petra Ilvonen:** Conceptualization; data curation; formal analysis; investigation; visualization; writing—original draft; writing—review and editing. **Reetta Pusa:** Formal analysis; investigation; resources. **Kai Härkönen:** Formal analysis; investigation; resources. **Saara Laitinen:** Conceptualization; funding acquisition; methodology; project administration; supervision; writing—review and editing. **Ulla Impola:** Conceptualization; data curation; formal analysis; investigation; methodology; supervision; writing—original draft; writing—review and editing.

## ACKNOWLEDGEMENTS

We would like to thank Birgitta Rantala and Lotta Andersson for their excellent technical assistance. We thank Pia Siljander and the personnel at the EV core unit and EV group of the University of Helsinki for providing laboratory facilities and assistance. We thank Mervi Lindman (EMBI) for technical assistance with SEM specimen preparation and the Electron Microscopy Unit of the Institute of Biotechnology of the University of Helsinki supported by Biocenter Finland for providing laboratory facilities. For technical assistance in cryoEM, we thank Behnam Lak and Pasi Laurinmäki of the Instruct-ERIC Centre Finland and the Biocenter Finland National Cryo-Electron Microscopy Unit, University of Helsinki. This work was supported by Business Finland Grant EVE Consortium 2346/31/2019.

## CONFLICT OF INTEREST STATEMENT

The authors declare no conflicts of interest.

## ORCID

Petra Ilvonen  <https://orcid.org/0000-0002-3711-9422>

## REFERENCES

- Aatonen, M. T., Öhman, T., Nyman, T. A., Laitinen, S., Grönholm, M., & Siljander, P. R. M. (2014). Isolation and characterization of platelet-derived extracellular vesicles. *Journal of Extracellular Vesicles*, 3(1), <https://doi.org/10.3402/jev.v3.24692>
- Anderson, H. L., Brodsky, I. E., & Mangalmurti, N. S. (2018). The evolving erythrocyte: Red blood cells as modulators of innate immunity. *Journal of Immunology*, 201(5), 1343–1351. <https://doi.org/10.4049/jimmunol.1800565>
- Arraud, N., Linares, R., Tan, S., Gounou, C., Pasquet, J. M., Mornet, S., & Brisson, A. R. (2014). Extracellular vesicles from blood plasma: Determination of their morphology, size, phenotype and concentration. *Journal of Thrombosis and Haemostasis*, 12(5), 614–627. <https://doi.org/10.1111/jth.12554>
- Burger, P., Hilarius-Stokman, P., De Korte, D., Van Den Berg, T. K., & Van Bruggen, R. (2012). CD47 functions as a molecular switch for erythrocyte phagocytosis. *Blood*, 119(23), 5512–5521. <https://doi.org/10.1182/blood-2011-10-386805>
- Butler, W. T. (1989). The nature and significance of osteopontin. *Connective Tissue Research*, 23(2-3), 123–136. <https://doi.org/10.3109/03008208909002412>
- Caillon, A., Trimaille, A., Favre, J., Jesel, L., Morel, O., & Kauffenstein, G. (2022). Role of neutrophils, platelets, and extracellular vesicles and their interactions in COVID-19-associated thrombopathy. *Journal of Thrombosis and Haemostasis*, 20(1), 17–31. <https://doi.org/10.1111/jth.15566>
- Chargaff, E., & West, R. (1946). The biological significance of the thromboplastic protein of blood. *Journal of Biological Chemistry*, 166(1), 189–197. [https://doi.org/10.1016/s0021-9258\(17\)34997-9](https://doi.org/10.1016/s0021-9258(17)34997-9)
- Danesh, A., Inglis, H. C., Jackman, R. P., Wu, S., Deng, X., Muench, M. O., Heitman, J. W., & Norris, P. J. (2014). Exosomes from red blood cell units bind to monocytes and induce proinflammatory cytokines, boosting T-cell responses *in vitro*. *Blood*, 123(5), 687–696. <https://doi.org/10.1182/blood-2013-10-530469>
- Dergunov, A. D., & Baserova, V. B. (2022). Different pathways of cellular cholesterol efflux. *Cell Biochemistry and Biophysics*, 80(3), 471–481. <https://doi.org/10.1007/s12013-022-01081-5>
- Di Trapani, M., Bassi, G., Midolo, M., Gatti, A., Kamga, P. T., Cassaro, A., Carusone, R., Adamo, A., & Krampera, M. (2016). Differential and transferable modulatory effects of mesenchymal stromal cell-derived extracellular vesicles on T, B and NK cell functions. *Scientific Reports*, 6, 24120. <https://doi.org/10.1038/srep24120>

- Dragovic, R. A., Gardiner, C., Brooks, A. S., Tannetta, D. S., Ferguson, D. J., Hole, P., Carr, B., Redman, C. W., Harris, A. L., Dobson, P. J., Harrison, P., & Sargent, I. L. (2011). Sizing and phenotyping of cellular vesicles using nanoparticle tracking analysis. *Nanomedicine: Nanotechnology, Biology and Medicine*, 7(6), 780–788. <https://doi.org/10.1016/j.nano.2011.04.003>
- Ebeyer-Masotta, M., Eichhorn, T., Weiss, R., Lauková, L., & Weber, V. (2022). Activated platelets and platelet-derived extracellular vesicles mediate COVID-19-associated immunothrombosis. *Frontiers in Cell and Developmental Biology*, 10, 1–11. <https://doi.org/10.3389/fcell.2022.914891>
- Gamonet, C., Desmarest, M., Mourey, G., Biichle, S., Aupet, S., Laheurte, C., François, A., Resch, E., Bigey, F., Binda, D., Bardiaux, L., Naegelen, C., Marpoux, N., Delettre, F. A., Saas, P., Morel, P., Tiberghien, P., Lacroix, J., Capellier, G., ... & Garnache-Ottou, F. (2020). Processing methods and storage duration impact extracellular vesicle counts in red blood cell units. *Blood Advances*, 4(21), 5527–5539. <https://doi.org/10.1182/bloodadvances.2020001658>
- Gamonet, C., Mourey, G., Aupet, S., Biichle, S., Petitjean, R., Vidal, C., Pugin, A., Naegelen, C., Tiberghien, P., Morel, P., Angelot-Delettre, F., Seilles, E., Saas, P., Bardiaux, L., & Garnache-Ottou, F. (2017). How to quantify microparticles in RBCs? A validated flow cytometry method allows the detection of an increase in microparticles during storage. *Transfusion*, 57(3), 504–516. <https://doi.org/10.1111/trf.13989>
- Görgens, A., Bremer, M., Ferrer-Tur, R., Murke, F., Tertel, T., Horn, P. A., Thalmann, S., Welsh, J. A., Probst, C., Guerin, C., Boulanger, C. M., Jones, J. C., Hanenberg, H., Erdbrügger, U., Lannigan, J., Ricklefs, F. L., El-Andaloussi, S., & Giebel, B. (2019). Optimisation of imaging flow cytometry for the analysis of single extracellular vesicles by using fluorescence-tagged vesicles as biological reference material. *Journal of Extracellular Vesicles*, 8(1), 1587567. <https://doi.org/10.1080/20013078.2019.1587567>
- Heidarzadeh, M., Gürsoy-Özdemir, Y., Kaya, M., Eslami Abriz, A., Zarebkohan, A., Rahbarghazi, R., & Sokullu, E. (2021). Exosomal delivery of therapeutic modulators through the blood–brain barrier; promise and pitfalls. *Cell & Bioscience*, 11(1), 1–28. <https://doi.org/10.1186/s13578-021-00650-0>
- Hemler, M. E. (2005). Tetraspanin functions and associated microdomains. *Nature Reviews. Molecular Cell Biology*, 6(10), 801–811. <https://doi.org/10.1038/nrm1736>
- Hewitt, R. E., Vis, B., Pele, L. C., Faria, N., & Powell, J. J. (2017). Imaging flow cytometry assays for quantifying pigment grade titanium dioxide particle internalization and interactions with immune cells in whole blood. *Cytometry: Part A*, 91(10), 1009–1020. <https://doi.org/10.1002/cyto.a.23245>
- Hottz, E. D., Azevedo-Quintanilha, I. G., Palhinha, L., Teixeira, L., Barreto, E. A., Pão, C. R. R., Righy, C., Franco, S., Souza, T. M. L., Kurtz, P., Bozza, F. A., & Bozza, P. T. (2020). Platelet activation and platelet-monocyte aggregate formation trigger tissue factor expression in patients with severe COVID-19. *Blood*, 136(11), 1330–1341. <https://doi.org/10.1182/blood.2020007252>
- Impola, U., Larjo, A., Salmenniemi, U., Putkonen, M., Ihl-Remes, M., & Partanen, J. (2016). Graft immune cell composition associates with clinical outcome of allogeneic etopetic stem cell transplantation in patients with AML. *Frontiers in Immunology*, 7, 1–10. <https://doi.org/10.3389/fimmu.2016.00523>
- Jenne, C. N., Urrutia, R., & Kubes, P. (2013). Platelets: Bridging hemostasis, inflammation, and immunity. *International Journal of Laboratory Hematology*, 35(3), 254–261. <https://doi.org/10.1111/ijlh.12084>
- Jurgielewicz, B. J., Yao, Y., & Stice, S. L. (2020). Kinetics and specificity of HEK293T extracellular vesicle uptake using imaging flow cytometry. *Nanoscale Research Letters*, 15(1), <https://doi.org/10.1186/s11671-020-03399-6>
- Kalluri, R., & LeBleu, V. S. (2020). The biology, function, and biomedical applications of exosomes. *Science*, 367(6478), <https://doi.org/10.1126/science.aau6977>
- Koponen, A., Kerkelä, E., Rojalín, T., Lázaro-Ibáñez, E., Suutari, T., Saari, H. O., Siljander, P., Yliperttula, M., Laitinen, S., & Viitala, T. (2020). Label-free characterization and real-time monitoring of cell uptake of extracellular vesicles. *Biosensors & Bioelectronics*, 168, 112510. <https://doi.org/10.1016/j.bios.2020.112510>
- Kowal, J., Arras, G., Colombo, M., Jouve, M., Paul, J., & Primald-bengtson, B. (2016). Proteomic comparison defines novel markers to characterize heterogeneous populations of extracellular vesicle subtypes. *PNAS*, 113(8), 968–977. <https://doi.org/10.1073/pnas.1521230113>
- Kralj-Iglič, V., Pocsfalvi, G., Mesarec, L., Šuštar, V., Hägerstrand, H., & Iglič, A. (2020). Minimizing isotropic and deviatoric membrane energy—an unifying formation mechanism of different cellular membrane nanovesicle types. *PLoS ONE*, 15(12), 1–25. <https://doi.org/10.1371/journal.pone.0244796>
- Kuo, W., Tigges, J., Toxavidis, V., & Ghiran, I. (2017). Red blood cells: A source of extracellular vesicle. *Methods in Molecular Biology*, 1660, 15–22. [https://doi.org/10.1007/978-1-4939-7253-1\\_2](https://doi.org/10.1007/978-1-4939-7253-1_2)
- Lai, S. J., Ohkawa, R., Horiuchi, Y., Kubota, T., & Tozuka, M. (2019). Red blood cells participate in reverse cholesterol transport by mediating cholesterol efflux of high-density lipoprotein and apolipoprotein A-I from THP-1 macrophages. *Biological Chemistry*, 400(12), 1593–1602. <https://doi.org/10.1515/hsz-2019-0244>
- Laurén, E., Sankkila, L., Pettilä, V., & Kerkelä, E. (2022). Immunomodulatory properties of packed red blood cells during storage. *Transfusion Medicine and Hemotherapy*, 1–10. <https://doi.org/10.1159/000525706>
- Laurén, E., Sankkila, L., Pettilä, V., & Kerkelä, E. (2022). Immunomodulatory properties of packed red blood cells during storage. *Transfusion Medicine and Hemotherapy : Offizielles Organ Der Deutschen Gesellschaft Fur Transfusionsmedizin Und Immunhamatologie*, 50(3), 208–217. <https://doi.org/10.1159/000525706>
- Laurén, E., Tigistu-Sahle, F., Valkonen, S., Westberg, M., Valkeajärvi, A., Eronen, J., Siljander, P., Pettilä, V., Käkälä, R., Laitinen, S., & Kerkelä, E. (2018). Phospholipid composition of packed red blood cells and that of extracellular vesicles show a high resemblance and stability during storage. *Biochim Biophys Acta—Mol Cell Biol Lipids*, 1863(1), 1–8. <https://doi.org/10.1016/j.bbalip.2017.09.012>
- Liu, Y. J., & Wang, C. (2023). A review of the regulatory mechanisms of extracellular vesicles-mediated intercellular communication. *Cell Communication and Signaling*, 21(1), 1–12. <https://doi.org/10.1186/s12964-023-01103-6>
- MacDonald, K. P. A., Munster, D. J., Clark, G. J., Dzionek, A., Schmitz, J., & Hart, D. N. J. (2002). Characterization of human blood dendritic cell subsets. *Blood*, 100(13), 4512–4520. <https://doi.org/10.1182/blood-2001-11-0097>
- Mantel, P. Y., Hjelmqvist, D., Walch, M., Kharoubi-Hess, S., Nilsson, S., Ravel, D., Ribeiro, M., Grüning, C., Ma, S., Padmanabhan, P., Trachtenberg, A., Ankarklev, J., Brancucci, N. M., Huttenhower, C., Duraisingh, M. T., Ghiran, I., Kuo, W. P., Filgueira, L., Martinelli, R., & Marti, M. (2016). Infected erythrocyte-derived extracellular vesicles alter vascular function via regulatory Ago2-miRNA complexes in malaria. *Nature Communications*, 7, 12727. <https://doi.org/10.1038/ncomms12727>
- Mathieu, M., Martin-Jaular, L., Lavie, G., & Théry, C. (2019). Specificities of secretion and uptake of exosomes and other extracellular vesicles for cell-to-cell communication. *Nature Cell Biology*, 21(1), 9–17. <https://doi.org/10.1038/s41556-018-0250-9>
- Mitchell, A. J., Pradel, L. C., Chasson, L., Van Rooijen, N., Grau, G. E., Hunt, N. H., & Chimini, G. (2010). Technical advance: Autofluorescence as a tool for myeloid cell analysis. *Journal of Leukocyte Biology*, 88(3), 597–603. <https://doi.org/10.1189/jlb.0310184>
- Mulcahy, L. A., Pink, R. C., & Carter, D. R. F. (2014). Routes and mechanisms of extracellular vesicle uptake. *Journal of Extracellular Vesicles*, 3(1), <https://doi.org/10.3402/jev.v3.24641>
- Németh, K., Varga, Z., Lenzinger, D., Visnovitz, T., Koncz, A., Hegedűs, N., Kittel, Á., Máthé, D., Szigeti, K., Lórinicz, P., O'Neill, C., Dwyer, R., Liu, Z., Buzás, E. I., & Tamási, V. (2021). Extracellular vesicle release and uptake by the liver under normo- and hyperlipidemia. *Cellular and Molecular Life Sciences*, 78(23), 7589–7604. <https://doi.org/10.1007/s00018-021-03969-6>
- Noris, M., & Galbusera, M. (2023). The complement alternative pathway and hemostasis. *Immunological Reviews*, 313(1), 139–161. <https://doi.org/10.1111/imr.13150>

- Onódi, Z., Pelyhe, C., Nagy, C. T., Brenner, G. B., & Almási, L. (2018). Isolation of high-purity extracellular vesicles by the combination of iodixanol density gradient ultracentrifugation and bind-elute chromatography from blood plasma. *Frontiers in Physiology*, 9, 1–11. <https://doi.org/10.3389/fphys.2018.01479>
- Palviainen, M., Saraswat, M., Varga, Z., Kitka, D., Neuvonen, M., Puhka, M., Joenväärä, S., Renkonen, R., Nieuwland, R., Takatalo, M., & Siljander, P. R. M. (2020). Extracellular vesicles from human plasma and serum are carriers of extravesicular cargo—implications for biomarker discovery. *PLoS ONE*, 15(8), 1–19. <https://doi.org/10.1371/journal.pone.0236439>
- Park, Y., Abihssira-García, I. S., Thalmann, S., Wiegertjes, G. F., Barreda, D. R., Olsvik, P. A., & Kiron, V. (2020). Imaging flow cytometry protocols for examining phagocytosis of microplastics and bioparticles by immune cells of aquatic animals. *Frontiers in Immunology*, 11, 203. <https://doi.org/10.3389/fimmu.2020.00203>
- Parkkila, P., Härkönen, K., Ilvonen, P., Laitinen, S., & Viitala, T. (2022). Protein A/G-based surface plasmon resonance biosensor for regenerable antibody-mediated capture and analysis of nanoparticles. *Colloids and Surfaces A: Physicochemical Engineering Aspects*, 654, 130015. <https://doi.org/10.1016/j.colsurfa.2022.130015>
- Passacquale, G., Vamadevan, P., Pereira, L., & Hamid, C., Corrigan, V., & Ferro, A. (2011). Monocyte-platelet interaction induces a pro-inflammatory phenotype in circulating monocytes. *PLoS ONE*, 6(10), <https://doi.org/10.1371/journal.pone.0025595>
- Puhm, F., Boilard, E., & MacHlus, K. R. (2021). Platelet extracellular vesicles; beyond the blood. *Arteriosclerosis, Thrombosis, and Vascular Biology*, 41(1), 87–96. <https://doi.org/10.1161/ATVBAHA.120.314644>
- Pužar Dominkuš, P., Stenovec, M., Sitar, S., Lasič, E., Zorec, R., Plemenitaš, A., Žagar, E., Kreft, M., & Lenassi, M. (2018). PKH26 labeling of extracellular vesicles: Characterization and cellular internalization of contaminating PKH26 nanoparticles. *Biochimica et Biophysica Acta—Biomembranes*, 1860(6), 1350–1361. <https://doi.org/10.1016/j.bbamem.2018.03.013>
- Qu, M., Lin, Q., Huang, L., Fu, Y., Wang, L., He, S., Fu, Y., Yang, S., Zhang, Z., Zhang, L., & Sun, X. (2018). Dopamine-loaded blood exosomes targeted to brain for better treatment of Parkinson's disease. *Journal of Controlled Release: Official Journal of the Controlled Release Society*, 287, 156–166. <https://doi.org/10.1016/j.jconrel.2018.08.035>
- Ratajczak, J., Wysoczynski, M., Hayek, F., Janowska-Wieczorek, A., & Ratajczak, M. Z. (2006). Membrane-derived microvesicles: Important and underappreciated mediators of cell-to-cell communication. *Leukemia*, 20, 1487–1495.
- Remy, K. E., Hall, M. W., Cholette, J., Juffermans, N. P., Nicol, K., Doctor, A., Blumberg, N., Spinella, P. C., Norris, P. J., Dahmer, M. K., & Muszynski, J. A., Pediatric Critical Care Blood Research Network (Blood Net). (2018). Mechanisms of red blood cell transfusion-related immunomodulation. *Transfusion*, 58(3), 804–815. <https://doi.org/10.1111/trf.14488>
- Robbins, P. D., & Morelli, A. E. (2014). Regulation of immune responses by extracellular vesicles. *Nature Immunology*, 14(3), 195–208. <https://doi.org/10.1038/nri3622.Regulation>
- Semple, J. W., Italiano, J. E., & Freedman, J. (2011). Platelets and the immune continuum. *Nature Reviews Immunology*, 11(4), 264–274. <https://doi.org/10.1038/nri2956>
- Shrirao, A. B., Schloss, R. S., Fritz, Z., Shrirao, M. V., Rosen, R., & Yarmush, M. L. (2021). Autofluorescence of blood and its application in biomedical and clinical research. *Biotechnology and Bioengineering*, 118(12), 4550–4576. <https://doi.org/10.1002/bit.27933>
- Sozzani, S., Del Prete, A., & Bosisio, D. (2017). Dendritic cell recruitment and activation in autoimmunity. *Journal of Autoimmunity*, 85, 126–140. <https://doi.org/10.1016/j.jaut.2017.07.012>
- Stachurska, A., Korsak, J., Gawe, D., & Trybus, W. (2019). Selected CD molecules and the phagocytosis of microvesicles released from erythrocytes ex vivo. *Vox Sanguinis*, 576–587. <https://doi.org/10.1111/vox.12819>
- Straat, M., van Hezel, M. E., Böing, A., Tuip-De Boer, A., Weber, N., Nieuwland, R., van Bruggen, R., & Juffermans, N. P. (2016). Monocyte-mediated activation of endothelial cells occurs only after binding to extracellular vesicles from red blood cell products, a process mediated by  $\beta$ -integrin. *Transfusion*, 56(12), 3012–3020. <https://doi.org/10.1111/trf.13851>
- Tertel, T., Görgens, A., & Giebel, B. (2020). Chapter four—analysis of individual extracellular vesicles by imaging flow cytometry. In S. Spada, & L. Galluzzi in E (Eds.), *Extracellular vesicles* (Vol. 645, pp. 55–78). Academic Press. <https://doi.org/10.1016/bs.mie.2020.05.013>
- Théry, C., Ostrowski, M., & Segura, E. (2009). Membrane vesicles as conveyors of immune responses. *Nature Reviews Immunology*, 9, 581–593.
- Théry, C., Zitvogel, L., & Amigorena, S. (2002). Exosomes: Composition, biogenesis and function. *Nature Reviews Immunology*, 2(8), 569–579. <https://doi.org/10.1038/nri855>
- Thierry, B., Chou, M. L., Goupran, H., Cognasse, F., Garraud, O., & Seghatchian, J. (2015). An overview of the role of microparticles/microvesicles in blood components: Are they clinically beneficial or harmful? *Transfusion and Apheresis Science*, 53(2), 137–145. <https://doi.org/10.1016/j.transci.2015.10.010>
- Tóth, E., Turiák, L., Visnovitz, T., Cserép, C., Mázló, A., Sódar, B. W., Försönits, A. I., Petővári, G., Sebestyén, A., Komlósi, Z., Drahos, L., Kittel, Á., Nagy, G., Bácsi, A., Dénes, Á., Gho, Y. S., Szabó-Taylor, K. É., & Buzás, E. I. (2021). Formation of a protein corona on the surface of extracellular vesicles in blood plasma. *Journal of Extracellular Vesicles*, 10(11). <https://doi.org/10.1002/jev2.12140>
- Valkonen, S., Mallas, B., Impola, U., Valkeajärvi, A., Eronen, J., Javela, K., Siljander, P. R., & Laitinen, S. (2019). Assessment of time-dependent platelet activation using extracellular vesicles, CD62P exposure, and soluble glycoprotein V content of platelet concentrates with two different platelet additive solutions. *Transfusion Medicine and Hemotherapy*, 46(4), 267–275. <https://doi.org/10.1159/000499958>
- van der Pol, E., Boing, A. N., Harrison, P., Sturk, A., & Nieuwland, R. (2012). Classification, functions, and clinical relevance of extracellular vesicles. *Pharmacological Reviews*, 64(3), 676–705. <https://doi.org/10.1124/pr.112.005983>
- Weiss, R., Gröger, M., Rauscher, S., Fendl, B., Eichhorn, T., Fischer, M. B., Spittler, A., & Weber, V. (2018). Differential interaction of platelet-derived extracellular vesicles with leukocyte subsets in human whole blood. *Scientific Reports*, 8(1), 6598. <https://doi.org/10.1038/s41598-018-25047-x>
- Yan, C., Wu, H., Fang, X., He, J., & Zhu, F. (2023). Platelet, a key regulator of innate and adaptive immunity. *Frontiers in Medicine*, 10, 1–11. <https://doi.org/10.3389/fmed.2023.1074878>
- Yáñez-Mó, M., Siljander, P. R. M., Andreu, Z., Zavec, A. B., Borràs, F. E., Buzas, E. I., Buzas, K., Casal, E., Cappello, F., Carvalho, J., Colás, E., Cordeiro-da Silva, A., Fais, S., Falcon-Perez, J. M., Ghobrial, I. M., Giebel, B., Gimona, M., Graner, M., Gursel, I., ... De Wever, O. (2015). Biological properties of extracellular vesicles and their physiological functions. *Journal of Extracellular Vesicles*, 4, 27066. <https://doi.org/10.3402/jev.v4.27066>
- Yates, A. G., Pink, R. C., Erdbrügger, U., Siljander, P. R., Dellar, E. R., Pantazi, P., Akbar, N., Cooke, W. R., Vatish, M., Dias-Neto, E., Anthony, D. C., & Couch, Y. (2022a). In sickness and in health: The functional role of extracellular vesicles in physiology and pathology in vivo: Part I: Health and normal physiology. *Journal of Extracellular Vesicles*, 11(1), e12151. <https://doi.org/10.1002/jev2.12151>
- Yates, A. G., Pink, R. C., Erdbrügger, U., Siljander, P. R., Dellar, E. R., Pantazi, P., Akbar, N., Cooke, W. R., Vatish, M., Dias-Neto, E., Anthony, D. C., & Couch, Y. (2022b). In sickness and in health: The functional role of extracellular vesicles in physiology and pathology in vivo: part II: Pathology. *Journal of Extracellular Vesicles*, 11(1), e12190. <https://doi.org/10.1002/jev2.12190>

Zhou, X., Xie, F., Wang, L., Zhang, L., Zhang, S., Fang, M., & Zhou, F. (2020). The function and clinical application of extracellular vesicles in innate immune regulation. *Cellular & Molecular Immunology*, 17(4), 323–334. <https://doi.org/10.1038/s41423-020-0391-1>

## SUPPORTING INFORMATION

Additional supporting information can be found online in the Supporting Information section at the end of this article.

**How to cite this article:** Ilvonen, P., Pusa, R., Härkönen, K., Laitinen, S., & Impola, U. (2024). Distinct targeting and uptake of platelet and red blood cell-derived extracellular vesicles into immune cells. *Journal of Extracellular Biology*, 3, e130. <https://doi.org/10.1002/jex2.130>